



Published in final edited form as:

Science. 2014 March 7; 343(6175): 1246980. doi:10.1126/science.1246980.

Common Genetic Variants Modulate Pathogen-Sensing Responses in Human Dendritic Cells

Mark N. Lee^{1,2,3,†}, **Chun Ye**^{1,†}, **Alexandra-Chloé Villani**^{1,2}, **Towfique Raj**^{1,2,4}, **Weibo Li**^{1,3}, **Thomas M. Eisenhaure**^{1,3}, **Selina H. Imboywa**², **Portia I. Chipendo**², **F. Ann Ran**^{1,5}, **Kamil Slowikowski**⁶, **Lucas D. Ward**^{1,7}, **Khadir Raddassi**⁸, **Cristin McCabe**^{1,2}, **Michelle H. Lee**², **Irene Y. Frohlich**², **David A. Hafler**⁸, **Manolis Kellis**^{1,7}, **Soumya Raychaudhuri**^{1,2,9,10}, **Feng Zhang**^{11,12,13}, **Barbara E. Stranger**^{14,15}, **Christophe O. Benoist**², **Philip L. De Jager**^{1,2,4}, **Aviv Regev**^{1,16,17,*}, and **Nir Hacohen**^{1,2,3,*}

¹Broad Institute of MIT and Harvard, Cambridge, MA 02142, USA

²Harvard Medical School, Boston, MA 02115, USA

³Center for Immunology and Inflammatory Diseases, Massachusetts General Hospital, Charlestown, MA 02129, USA

⁴Program in Translational NeuroPsychiatric Genomics, Department of Neurology, Brigham & Women's Hospital, Boston MA 02115, USA

⁵Department of Molecular and Cellular Biology, Harvard University, Cambridge, MA 02138, USA

⁶Bioinformatics and Integrative Genomics, Graduate School of Arts and Sciences, Harvard University, Cambridge, MA 02138, USA

⁷Computer Science and Artificial Intelligence Laboratory, Massachusetts Institute of Technology, Cambridge, MA 02139, USA

⁸Department of Neurology, Yale School of Medicine, CT 06511, USA

⁹Divisions of Genetics and Rheumatology, Department of Medicine, Brigham and Women's Hospital, Boston, MA 02115, USA

¹⁰Arthritis Research UK Epidemiology Unit, Musculoskeletal Research Group, University of Manchester, Manchester Academic Health Sciences Centre, UK

¹¹McGovern Institute for Brain Research, MIT, Cambridge, MA, 02139, USA

¹²Department of Brain and Cognitive Sciences, MIT, Cambridge, MA, 02139, USA

¹³Department of Biological Engineering, MIT, Cambridge, MA, 02139, USA

¹⁴Section of Genetic Medicine, The University of Chicago, Chicago, IL 60637, USA

*Correspondence to: aregev@broad.mit.edu, nhacohen@partners.org.

†These authors contributed equally to this work.

Supplementary Materials: Materials and Methods

Supplementary Text

Figs. S1 to S5

Tables S1 to S11

References (46-72)

¹⁵Institute for Genomics and Systems Biology, The University of Chicago, Chicago, IL 60637, USA

¹⁶Department of Biology, Massachusetts Institute of Technology, Cambridge, MA 02139, USA

¹⁷Howard Hughes Medical Institute

Abstract

Little is known about how human genetic variation affects the responses to environmental stimuli in the context of complex diseases. Experimental and computational approaches were applied to determine the effects of genetic variation on the induction of pathogen-responsive genes in human dendritic cells. We identified 121 common genetic variants associated in *cis* with variation in expression responses to *E. coli* lipopolysaccharide, influenza or interferon- β (IFN β). We localized and validated causal variants to binding sites of pathogen-activated STAT and IRF transcription factors. We also identified a common variant in *IRF7* that is associated in *trans* with type I interferon induction in response to influenza infection. Our results reveal common alleles that explain inter-individual variation in pathogen sensing and provide functional annotation for genetic variants that alter susceptibility to inflammatory diseases.

Introduction

Susceptibility to complex diseases depends on both genetic predisposition and exposure to environmental factors, with interactions between the two (GxE interactions) likely contributing substantially to disease risk (1, 2). However, the extent and mechanisms by which common human genetic variants interact with the environment remain poorly explored and have been difficult to detect in clinical studies (1, 3). Genetic analysis of molecular traits – such as gene expression profiles – offers a promising way to dissect the molecular mechanisms underlying GxE interactions. Expression quantitative trait locus (eQTL) studies have been used to map genetic variants contributing to variation in gene expression, but have largely focused on steady state expression in humans (4, 5), thus excluding GxE interactions. In model organisms, differences in growth conditions or treatment with various stimuli have revealed the existence of response eQTLs (reQTLs) (6-9), defined as QTLs associated with the change in expression after stimulation. Here, we sought to identify reQTLs in humans, to explain the mechanism by which the environment interacts with these variants, and to determine whether these variants are associated with immune-mediated diseases.

We used dendritic cells (DCs) of the innate immune system as a model system for reQTL studies, with physiological and clinical relevance. DCs play a direct role in the host recognition of pathogens using specialized sensors that engage well-characterized signaling and transcriptional networks. For example, bacterial lipopolysaccharide (LPS) activates two distinct arms of the Toll-like receptor 4 (TLR4) pathway, whereas influenza infection primarily activates the RNA-sensing Toll-like receptors (e.g., TLR3) and the RIG-I-like receptors (e.g., RIG-I) (10). These, in turn, lead to the translocation of transcription factors from the cytoplasm into the nucleus to induce the expression of immune genes, including IFN β secretion that engages the type I interferon response pathway to induce the expression

of hundreds of anti-viral effectors. Genetic studies have associated common variants near many genes in these pathways with risk of different inflammatory diseases (11, 12). DCs also play a critical role in the pathologic immune responses underlying inflammatory diseases (11-13), also reflected in recent genome-wide association studies (GWAS) of several diseases (14-17), especially inflammatory bowel disease (14).

Results

Assessing the impact of genetic variation on pathogen-sensing in primary human DCs

We developed an integrated experimental and computational pipeline (Fig. 1A) to identify variability in human DC responses and associate this variability with common genetic variants. First, we optimized a high-throughput protocol to isolate primary CD14⁺CD16^{lo} monocytes from human blood samples (figs. S1A–S1F), differentiate them into monocyte-derived dendritic cells (MoDCs), and stimulate them with three immunostimulatory agents (Fig. 1B): *E. coli* lipopolysaccharide (LPS), influenza virus, or IFN β (a cytokine induced by LPS and influenza). Second, we collected genome-wide transcript profiles from resting and stimulated DCs from 30 healthy individuals and computationally identified a ‘signature’ of 415 genes that would be informative of variation in the response in a larger cohort. Third, we generated 1,598 transcriptional profiles (using an amplification-free platform suitable for small cell numbers (18)) from DCs isolated from 534 healthy individuals (295 Caucasians, 122 African-Americans, 117 East Asians; table S1) in four states: resting, LPS-stimulated, influenza-infected and IFN β -stimulated. Finally, we associated expression variation with genetic variation to identify *cis*- and *trans*-eQTLs and reQTLs, and investigated candidate reQTLs for their mechanism of action.

Variability of pathogen-sensing responses between individuals

To assess the inter-individual variability of DC responses, we first profiled genome-wide expression using microarrays in resting, LPS-stimulated and influenza-infected MoDCs isolated from each of 30 healthy individuals (18 Caucasians, 6 Asians, 6 African-Americans). We found 1,413 genes that were regulated in LPS- or influenza-treated cells [$\log_2(\text{fold change}) > 0.75$ or < -1.5 ; FDR < 0.01 ; fig. S2A, table S2A; see table S2B–I for enriched biological processes] at 5 hrs and 10 hrs, respectively (time points selected to have maximal expression of induced clusters; figs. S1B and S1C).

We quantified reproducibility in these responses by recalling 12 of the 30 donors 2-9 months after the first collection for MoDC isolations and profiling (table S1); we identified genes whose inter-individual expression variance is significantly higher than their intra-individual variance based on the serial replicates (taking into account known covariates including gender, age and population and unknown ones using Surrogate Variable Analysis (SVA) (19)). 222 of the 1,413 regulated genes (16%) showed significantly higher (FDR < 0.1) inter- than intra-individual variability, either in their absolute expression or in the differential expression (stimulated/baseline level) to at least one stimulus (Fig. 2A and table S3). These results suggest that there is consistent variation in these traits that may have a genetic basis.

Expression profiling of a pathogen response signature

Mapping the genetic basis of inter-individual variation in pathogen responses requires profiling of DC gene expression in a larger cohort; this poses a substantial technical challenge given the limited numbers of primary cells and multiple stimuli. Furthermore, the responses of DCs to virus, bacterial ligands and interferon are limited in scope, and do not encompass the entire genome. We therefore defined a 415 gene signature set (Fig. 2B and table S3) that could be monitored in small numbers of cells using a sensitive multiplex RNA detection system (18), allowing us to scale up our study. The signature consisted of: (1) all 222 of 1,413 regulated genes with greater inter- than intra-individual variability in the microarray study; (2) all 24 regulated genes exhibiting greater inter- than intra-population variability (FDR < 0.1; table S3) in the microarray study; (3) 76 genes comprising the known components of the TLR4, TLR3, RIG-I and IFNAR pathways (Fig. 1B) (10, 20-22); (4) 61 regulated genes that play key roles in the DC response (e.g. *IFNB1* and *IFITM3*) (22-24); (5) 28 regulated genes residing in loci previously associated with autoimmune or infectious diseases (25); and (6) 35 control genes including those that had among the lowest inter-individual variance in the microarray profiles. This representative signature allowed us to monitor genes with high inter-individual variability, as well as key components and responses of the pathogen-sensing pathway.

We then generated 1,598 transcriptional profiles, using the 415-gene signature, from MoDCs isolated from 534 healthy individuals (and 37 serially-collected replicates) in up to four conditions: resting (528 individuals), LPS-stimulated (356), influenza-infected (342) and IFN β -stimulated (284) (Figs. 2C, S1E, S1F, table S1). The IFN β stimulus allowed us to partition genes that were induced by both LPS and influenza (cluster III) into those induced secondary to type I IFN signaling (cluster IIIa) or by other mechanisms shared between these bacterial and viral sensing pathways (cluster IIIb) such as NF- κ B or AP-1 activation (Figs. 2C and 1B). The signature expression profiles clustered similarly to those from the microarray analysis (Fig. 2C and fig. S2C), and captured most of the variance in the genome-wide profile (cross validation, >0.99 gtPCC; fig. S2D (26)), demonstrating the utility of the signature to capture the genome-wide response.

reQTLs modulate cellular responses to pathogens

We mapped *cis*-eQTLs and *cis*-reQTLs by testing for association between common SNPs (minor allele frequency >5%; genotyped with Illumina Human OmniExpress BeadChip) and variation in either absolute transcript abundance (eQTL) or stimulation-induced change in transcript abundance (reQTL) in a nearby gene (in which the transcriptional start site or stop codon is within 1Mb of the SNP). We pooled individuals from the three human populations together and included covariates and principal components to increase statistical power while avoiding systematic confounders such as population structure and expression heterogeneity. We identified 264 genes with *cis*-eQTLs in at least one condition (permutation FDR < 0.05; Fig. 3A, figs. S3A–C, table S4A–D) (27). Notably, 22/264 genes also associated with additional independent *cis*-eQTLs after conditioning on the top five most significant SNPs in each *cis*-eQTL region (table S6 and fig. S3D) (27), reflecting the complexity of the regulatory landscape around each gene.

We detected 121 *cis*-reQTLs (Fig. 3B and table S4E–G; permutation FDR < 0.05; 91% internal reproducibility in at least 2 human populations, table S5), the subset of genetic variants that affect the induction of gene expression by LPS, influenza or IFN β . Of the 121 genes with *cis*-reQTLs, 7 associations were found only in the influenza condition (e.g., *IFNA21*, Fig. 3C and fig. S3B; meta-analysis, $P < 1 \times 10^{-5}$, permutation FDR 0.02–0.03), 15 in both the LPS and influenza conditions (e.g., *TEC*; Figs. 3C and S3B), and 57 in all three stimulation conditions (e.g. *ARL5B*, *SLFN5*, *CLEC4F*; Figs. 3C–3E and S3B), likely reflecting activation of the shared IFN β pathway. We hypothesized that causal variants driving *cis*-reQTLs alter the sequence of genomic elements that respond to transcription factors downstream of the pathogen-sensing receptors (Fig. 3F), and represent gene-by-environment interactions.

To validate *cis*-reQTLs, we quantified allele-specific expression for pan-stimulation-specific associations in heterozygote individuals (Figs. 3D and 3E). This was feasible for a gene with an exonic SNP (*CLEC4F* rs2075221) that was the most significant reQTL SNP, and for a gene with an exonic SNP (*SLFN5* rs11651240) in linkage disequilibrium (LD) with the most significant reQTL SNP (rs11867191, $R^2 = 0.501$ CEU). As predicted, transcripts derived from the major and minor alleles differed in expression after stimulation with LPS (*SLFN5*, $P < 0.001$, t-test; *CLEC4F*, $P < 0.01$), influenza (*SLFN5*, $P < 0.001$; *CLEC4F*, $P < 0.01$) or IFN β (*SLFN5*, $P < 0.001$; *CLEC4F*, $P < 0.001$) but not at baseline (Figs. 3D and 3E).

***cis*-reQTLs that alter the sequence of TF binding sites**

We hypothesized that the causal variants underlying *cis*-reQTLs functionally alter the chromosomal binding sites of transcription factors activated by one or more stimuli. To fine map reQTLs, we performed a *trans*-ethnic meta-analysis (28) of imputed variants in each population (~10M). We then examined whether the most highly associated meta-reQTLs overlap with transcription factor (TF) binding sites identified in high-throughput human ChIP-Seq datasets (e.g., ENCODE) or computationally-predicted conserved regulatory elements (29–31). We found substantial enrichment (table S7) of known binding sites for TFs from the STAT family (TFs that are known to be activated downstream of Type I IFN signaling). The most significant enrichment over background was found for STAT2 (116-fold, binomial $P < 2.55 \times 10^{-21}$) and STAT1 (126-fold, binomial $P < 2.98 \times 10^{-13}$) binding sites (derived from ChIP-seq in IFN α -stimulated K562 cells) within *cis*-eQTLs after IFN β stimulation.

Among the 57 genes (e.g., *SLFN5*, *CLEC4F*, *ARL5B*; Fig. 3F) with *cis*-reQTLs in all 3 stimuli, we observed that the most significant *cis*-reQTL in the: (1) *SLFN5* locus (rs11080327) lies in an ENCODE ChIP-Seq signal (29) for STAT1 (Figs. 4A–C); (2) *CLEC4F* locus (rs35856355) alters a commonly occurring cytosine in a canonical ISRE (interferon-stimulated response element) that is a target of IFN-activated transcription factors (Figs. 4B and 4C) (22, 30–32); and (3) *ARL5B* locus (rs2130531) changes a guanine in the canonical ISRE motif (Figs. 4B and 4C). Additional *cis*-reQTLs that alter putative STAT binding sites based on ChIP-Seq data or predicted ISRE motifs include: rs10086852 (*PTK2B*), rs1981760 (*NOD2*), rs73023464 (*C19ORF12*), rs1331717 (*IFI44*) and rs12064196 (*IFI44*) (Fig. 4A). Because STAT transcription factors are activated downstream of the type

IFN receptor (IFNAR) and bind to ISRE motifs (Fig. 4A) (22), we hypothesized that the SNPs in these sites are likely causal SNPs within their respective *cis*-reQTL regions.

***cis*-reQTLs affect differential binding of stimulus-activated transcription factors**

To experimentally validate our predicted regulatory mechanisms, we determined whether IFN β -activated transcription factors bind differentially at these SNPs. Using radiolabeled 24-26 bp dsDNA probes in electrophoretic mobility shift assays (EMSA), we found that probes encompassing the major alleles (rs35856355^C and rs2130531^G, which are associated with increased expression in *CLEC4F* and *ARL5B*), but not the minor alleles, shifted after incubation with IFN β -stimulated MoDC nuclear lysates (Fig. 4D). Consistently, non-radiolabeled major but not minor allele probes competed for binding to the IFN β -stimulated nuclear factors (fig. S4A). By incubating with antibodies to transcription factors known to bind the ISRE element, we found that IRF1 super-shifted the low MW band and STAT2 and IRF9 super-shifted the higher MW band, consistent with the known complex of these latter two proteins (32) (Fig. 4D). These results suggested that the SNPs in *CLEC4F* and *ARL5B* alter the binding of IFN-activated IRF1, STAT2 and IRF9 transcription factors.

To directly test the functional effects of the SNPs, we cloned 150-200 bp genomic regions surrounding rs11080327 (*SLFN5*), rs35856355 (*CLEC4F*) and rs2130531 (*ARL5B*) upstream of a luciferase reporter driven by a minimal promoter (Fig. 4E). For each region, we created two constructs that differ only at the respective SNPs. Since almost all cell types respond to IFN β stimulation, we transfected the reporter constructs into HEK-293 cells and stimulated the cells with IFN β . Consistent with our hypothesis, the constructs containing the major alleles of rs11080327 (*SLFN5*), rs35856355 (*CLEC4F*) and rs2130531 (*ARL5B*) induced respectively 11.6-fold, 2.1-fold and 1.5-fold more luciferase production than the cognate constructs containing the minor alleles (t-test, $P < 0.001$, $P < 0.001$ and $P < 0.01$, respectively; Fig. 4E). Furthermore, mutation of motif-conserving nucleotides across the *CLEC4F* ISRE motif reduced induction by IFN β while mutation of non-conserved nucleotides did not (fig. S4B), consistent with the ISRE consensus motif.

Finally, to further test (33) the functionality of rs11080327 – the *SLFN5* variant with the strongest functional effect – in its native chromosome, we directly edited the genome using the CRISPR system (34, 35), converting the heterozygous rs11080327^{A/G} in HEK-293 cells to a homozygous rs11080327^{G/G} (Fig. 4F and fig. S4C). We then stimulated both native and CRISPR-converted cells with IFN β . The fold induction of *SLFN5* decreased from 3.64 in heterozygous cells to 1.03 in the converted rs11080327 (G) homozygotes, while the induction of other genes was unaffected (Fig. 4F and fig. S4C).

The enrichment, EMSA, reporter assays and directed mutagenesis results suggest that we have identified causal variants in some of these *cis*-reQTL regions and demonstrate that the reQTLs occur due to differential binding of stimulus-activated transcription factors.

A *cis*-eQTL associating with *IRF7* is a *trans*-reQTL

We next attempted to detect cases where variation in gene expression is explained by distant genetic variants acting in *trans*. We noted that *cis*-eQTLs for regulator genes tend to have

smaller effect sizes and less significant *P*-values than those for regulated genes (fig. S3E). To decrease the multiple testing burden of detecting *trans* associations, we restricted testing SNPs local to genes on our gene signature set. A number of these are *cis*-eQTLs associated with the expression of genes encoding regulators (*e.g.*, transcription factors) in pathways that we stimulated (Fig. 5A). Of these, rs12805435 was the most significant, associating with the expression of the master anti-viral transcription factor *IRF7* in *cis* only after influenza, LPS or IFN β stimulation (table S4A–D). This SNP associated with both the expression and induction of 7 additional genes in *trans* (*i.e.* the transcriptional start site or stop codon is located > 1 Mb from the SNP) only after influenza infection: *NMI*, *IFNA4*, *IFNA10*, *IFNA13*, *IFNA21*, *IFNA17* and *IFNA5* ($P < 6.26 \times 10^{-5}$ in expression, $P < 1.68 \times 10^{-5}$ in differential expression; Fig. 5B and table S8–10).

To test whether the *trans*-associated genes are indeed targets of *IRF7*, we infected MoDCs that overexpressed *IRF7* or a control gene with influenza virus, and found that *IRF7* overexpression induced the expression of *IFNA2*, *IFNA13* and *IFNA14* in influenza-infected cells (Fig. 5C). In addition, in HEK-293 cells, which normally express very low levels of *IRF7*, we overexpressed *IRF7* and observed induction of *NMI*, *IFNA4*, *IFNA10*, *IFNA13*, *IFNA14* and *IFNA21* (Fig. 5D), suggesting that *IRF7* is sufficient to drive downstream expression. We have thus identified a stimulus-specific *cis*-eQTL associated with *IRF7* expression, which is also a *trans*-reQTL that underlies the variability of IFN induction in response to influenza infection in humans.

reQTLs in DCs overlap with autoimmune and infectious disease SNPs from GWAS

We examined the subset of loci associated in genome-wide association studies (GWAS) with inflammatory disorders. We first extended an analysis of Crohn's disease in which loci are enriched for genes specifically expressed in DCs (12, 14) to multiple sclerosis, celiac disease, psoriasis and leprosy (fig. S5A). We found that genes nearest to the susceptibility loci for these diseases were not only enriched in DC-specific genes but also in genes induced by LPS and/or influenza (fig. S5B), suggesting that some of the GWAS loci modulate the expression of the corresponding genes in activated DCs.

Supporting this hypothesis, 15 *cis*-reQTLs and 23 *cis*-eQTLs that were not significant at baseline but only became significant after stimulation are the same SNPs previously identified in GWAS of autoimmune and infectious diseases, including Crohn's disease, multiple sclerosis, celiac disease, psoriasis and leprosy (25) (Figs. 6A, 6B and table S11). These include: *NOD2* with leprosy (rs9302752), *IRF7* with systemic lupus erythematosus (rs4963128), *TRAF1* with rheumatoid arthritis (rs881375), and *CREM* with Crohn's disease (rs12242110) and ulcerative colitis (rs4246905). For example, rs9302752 – a SNP previously associated with susceptibility to leprosy (17) – was associated in our study with expression of *NOD2* and its response under IFN β stimulation ($P = 3.49 \times 10^{-25}$) but not at baseline (Fig. 6A and table S11); *NOD2* plays a known role in pathogen sensing and possibly mycobacterial immunity (36). Similarly, rs4963128 – a variant associated with SLE (37) – was associated in our study with the expression of *IRF7* after IFN β stimulation ($P = 1.10 \times 10^{-16}$) but not at baseline (Fig. 6A), in line with the importance of type I IFN responses in SLE pathogenesis (38). We note that rs4963128 is on the same haplotype ($R^2 =$

0.69, $D' = 0.94$) as the *IRF7* SNP rs12805435 that is associated with the *trans*-reQTL effect described above. These results suggest a role for innate immune pathogen-sensing pathways in the pathogenesis of these inflammatory disorders.

Discussion

While genetic association studies have identified alleles that confer disease risk, little is known about how these genetic variants contribute to disease through their effects on specific biological processes and their interaction with environmental stimuli. We addressed this question by quantifying the dendritic cell response to pathogens in a set of genotyped individuals, and then leveraged our understanding of these pathways to explain the mechanisms underlying the observed genotype-environment-phenotype interactions.

Many of the QTL associations we identified are only detectable in the presence of specific stimuli, underscoring the need to activate cells to capture additional genotype-phenotype relationships (39-41). Furthermore, few eQTL studies have definitively identified the causal variants underlying the associations. By measuring variability in hundreds of individuals, applying stimuli that partially overlap in their downstream pathways, and leveraging genomic datasets such as the 1000 Genomes Project and ENCODE (29, 42), we (i) pinpointed causal variants in reQTL regions and (ii) identified the stimulus-activated transcription factors that bind differentially at these SNPs, explaining some of the GxE interactions. Our dataset can thus be used to explore mechanisms of GxE interactions (43) and are consistent with DNaseI-sensitivity QTL (44) and ChIP-Seq QTL (45) studies that showed that differential transcription factor binding between individuals is pervasive in resting cells.

The reQTLs we identified provide genetic explanations for inter-individual variation in innate immune responses. This is best exemplified by the *trans*-reQTL in the *IRF7* locus that regulates the type I IFN anti-viral response. Our study reveals the effects of this *trans*-reQTL on target genes (anti-viral IFN module) in the context of a particular cell type (DCs) and in response to specific ligands (influenza). The changes in this immune response are, in turn, likely to impact organismal phenotypes that are driven by the IFN module, including susceptibility to viral infections and autoimmune diseases like SLE.

Overall, our high-throughput experimental pipeline and integrative analysis of primary human dendritic cells reveals abundant gene-by-environment interactions, points to the effects of disease variants on pathogen detection, and motivates extending our approach to a wide variety of immune cell types and stimulatory conditions to better explain the impact of human genetic variation on the immune response.

Supplementary Material

Refer to Web version on PubMed Central for supplementary material.

Acknowledgments

We thank all study participants in the PhenoGenetic project for their contributions. We are grateful to Q. Sievers and C. Wu for advice about preparing primary cells and V. Agarwala and D. A. Landau for valuable discussions.

This work was supported by the National Institute of General Medical Sciences, NIH, grant RC2 GM093080 (C.O.B. and N.H.); the National Institute of Allergy and Infectious Diseases grant U19 AI082630 and NIH Director's New Innovator Award DP2 OD002230 (N.H.); the National Human Genome Research Institute grant P50 HG006193, NIH Director's Pioneer Award DP1 CA174427, and Howard Hughes Medical Institute (A.R.); and NIH grant R01 HG004037 (M.K.). F.Z. is supported by an NIH Director's Pioneer Award (DP1 MH100706), an NIH Transformative R01 grant (R01 DK097768), the Keck, McKnight, Merkin, Vallee, Damon Runyon, Searle Scholars, Klingenstein, and Simons Foundations, Bob Metcalfe, and Jane Pauley. M.N.L. is supported by the NIH Medical Scientist Training Program fellowship (T32 GM007753). T.R. is supported by NIH fellowship F32 AG043267. K.S. is supported by NIH grant T32 HG002295. Gene expression data are deposited in NCBI's Gene Expression Omnibus under accession no. GSE57542.

References

1. Civelek M, Lusis AJ. Systems genetics approaches to understand complex traits. *Nature reviews Genetics*. Dec 3.2013
2. Thomas D. Gene--environment-wide association studies: emerging approaches. *Nature reviews Genetics*. Apr.2010 11:259.
3. Eichler EE, et al. Missing heritability and strategies for finding the underlying causes of complex disease. *Nature reviews Genetics*. Jun.2010 11:446.
4. Stranger BE, et al. Population genomics of human gene expression. *Nature genetics*. Oct.2007 39:1217. [PubMed: 17873874]
5. Schadt EE, et al. Genetics of gene expression surveyed in maize, mouse and man. *Nature*. Mar 20.2003 422:297. [PubMed: 12646919]
6. Gat-Viks I, et al. Deciphering molecular circuits from genetic variation underlying transcriptional responsiveness to stimuli. *Nature biotechnology*. Apr.2013 31:342.
7. Orozco LD, et al. Unraveling inflammatory responses using systems genetics and gene-environment interactions in macrophages. *Cell*. Oct 26.2012 151:658. [PubMed: 23101632]
8. Smith EN, Kruglyak L. Gene-environment interaction in yeast gene expression. *PLoS biology*. Apr 15.2008 6:e83. [PubMed: 18416601]
9. Li Y, et al. Mapping determinants of gene expression plasticity by genetical genomics in *C. elegans*. *PLoS genetics*. Dec 29.2006 2:e222. [PubMed: 17196041]
10. Takeuchi O, Akira S. Pattern recognition receptors and inflammation. *Cell*. Mar 19.2010 140:805. [PubMed: 20303872]
11. Rai E, Wakeland EK. Genetic predisposition to autoimmunity--what have we learned? *Seminars in immunology*. Apr.2011 23:67. [PubMed: 21288738]
12. Hu X, et al. Integrating autoimmune risk loci with gene-expression data identifies specific pathogenic immune cell subsets. *American journal of human genetics*. Oct 7.2011 89:496. [PubMed: 21963258]
13. Merad M, Sathe P, Helft J, Miller J, Mortha A. The dendritic cell lineage: ontogeny and function of dendritic cells and their subsets in the steady state and the inflamed setting. *Annu Rev Immunol*. 2013; 31:563. [PubMed: 23516985]
14. Jostins L, et al. Host-microbe interactions have shaped the genetic architecture of inflammatory bowel disease. *Nature*. Nov 1.2012 491:119. [PubMed: 23128233]
15. Tsoi LC, et al. Identification of 15 new psoriasis susceptibility loci highlights the role of innate immunity. *Nature genetics*. Dec.2012 44:1341. [PubMed: 23143594]
16. Thomas DL, et al. Genetic variation in IL28B and spontaneous clearance of hepatitis C virus. *Nature*. Oct 8.2009 461:798. [PubMed: 19759533]
17. Zhang FR, et al. Genomewide association study of leprosy. *The New England journal of medicine*. Dec 31.2009 361:2609. [PubMed: 20018961]
18. Geiss GK, et al. Direct multiplexed measurement of gene expression with color-coded probe pairs. *Nature biotechnology*. Mar.2008 26:317.
19. Leek JT, Storey JD. Capturing heterogeneity in gene expression studies by surrogate variable analysis. *PLoS genetics*. Sep.2007 3:1724. [PubMed: 17907809]
20. Kawai T, Akira S. The role of pattern-recognition receptors in innate immunity: update on Toll-like receptors. *Nature immunology*. May.2010 11:373. [PubMed: 20404851]

21. Barbalat R, Ewald SE, Mouchess ML, Barton GM. Nucleic acid recognition by the innate immune system. *Annu Rev Immunol.* 2011; 29:185. [PubMed: 21219183]
22. Stark GR, Kerr IM, Williams BR, Silverman RH, Schreiber RD. How cells respond to interferons. *Annual review of biochemistry.* 1998; 67:227.
23. Brass AL, et al. The IFITM proteins mediate cellular resistance to influenza A H1N1 virus, West Nile virus, and dengue virus. *Cell.* Dec 24.2009 139:1243. [PubMed: 20064371]
24. Everitt AR, et al. IFITM3 restricts the morbidity and mortality associated with influenza. *Nature.* Apr 26.2012 484:519. [PubMed: 22446628]
25. Hindorf LA, MJ.; Morales, J.; Junkins, HA.; Hall, PN.; Klemm, AK.; Manolio, TA. [Accessed 06/01/2013] A Catalog of Published Genome-Wide Association Studies. Available at: <http://www.genome.gov/gwastudies>
26. Donner Y, Feng T, Benoist C, Koller D. Imputing gene expression from selectively reduced probe sets. *Nature methods.* Nov.2012 9:1120. [PubMed: 23064520]
27. Supplementary text is available on *Science* Online.
28. Han B, Eskin E. Random-effects model aimed at discovering associations in meta-analysis of genome-wide association studies. *American journal of human genetics.* May 13.2011 88:586. [PubMed: 21565292]
29. ENCODE Project Consortium. An integrated encyclopedia of DNA elements in the human genome. *Nature.* Sep 6.2012 489:57. [PubMed: 22955616]
30. Ward LD, Kellis M. HaploReg: a resource for exploring chromatin states, conservation, and regulatory motif alterations within sets of genetically linked variants. *Nucleic acids research.* Jan. 2012 40:D930. [PubMed: 22064851]
31. Boyle AP, et al. Annotation of functional variation in personal genomes using RegulomeDB. *Genome research.* Sep.2012 22:1790. [PubMed: 22955989]
32. Honda K, Taniguchi T. IRFs: master regulators of signalling by Toll-like receptors and cytosolic pattern-recognition receptors. *Nature reviews Immunology.* Sep.2006 6:644.
33. Mackay TF, Stone EA, Ayroles JF. The genetics of quantitative traits: challenges and prospects. *Nature reviews Genetics.* Aug.2009 10:565.
34. Cong L, et al. Multiplex genome engineering using CRISPR/Cas systems. *Science.* Feb 15.2013 339:819. [PubMed: 23287718]
35. Mali P, et al. RNA-guided human genome engineering via Cas9. *Science.* Feb 15.2013 339:823. [PubMed: 23287722]
36. Divangahi M, et al. NOD2-deficient mice have impaired resistance to *Mycobacterium tuberculosis* infection through defective innate and adaptive immunity. *Journal of immunology.* Nov 15.2008 181:7157.
37. International Consortium for Systemic Lupus Erythematosus. Genome-wide association scan in women with systemic lupus erythematosus identifies susceptibility variants in ITGAM, PXX, KIAA1542 and other loci. *Nature genetics.* Feb.2008 40:204. [PubMed: 18204446]
38. Pascual V, Chaussabel D, Banchereau J. A genomic approach to human autoimmune diseases. *Annu Rev Immunol.* 2010; 28:535. [PubMed: 20192809]
39. Smirnov DA, Morley M, Shin E, Spielman RS, Cheung VG. Genetic analysis of radiation-induced changes in human gene expression. *Nature.* May 28.2009 459:587. [PubMed: 19349959]
40. Romanoski CE, et al. Systems genetics analysis of gene-by-environment interactions in human cells. *American journal of human genetics.* Mar 12.2010 86:399. [PubMed: 20170901]
41. Barreiro LB, et al. Deciphering the genetic architecture of variation in the immune response to *Mycobacterium tuberculosis* infection. *Proceedings of the National Academy of Sciences of the United States of America.* Jan 24.2012 109:1204. [PubMed: 22233810]
42. 1000 Genomes Project Consortium. An integrated map of genetic variation from 1,092 human genomes. *Nature.* Nov 1.2012 491:56. [PubMed: 23128226]
43. Stower H. Gene regulation: From genetic variation to phenotype via chromatin. *Nature reviews Genetics.* Dec.2013 14:824.
44. Degner JF, et al. DNase I sensitivity QTLs are a major determinant of human expression variation. *Nature.* Feb 16.2012 482:390. [PubMed: 22307276]

45. Kasowski M, et al. Variation in transcription factor binding among humans. *Science*. Apr 9.2010 328:232. [PubMed: 20299548]

Author Manuscript

Author Manuscript

Author Manuscript

Author Manuscript

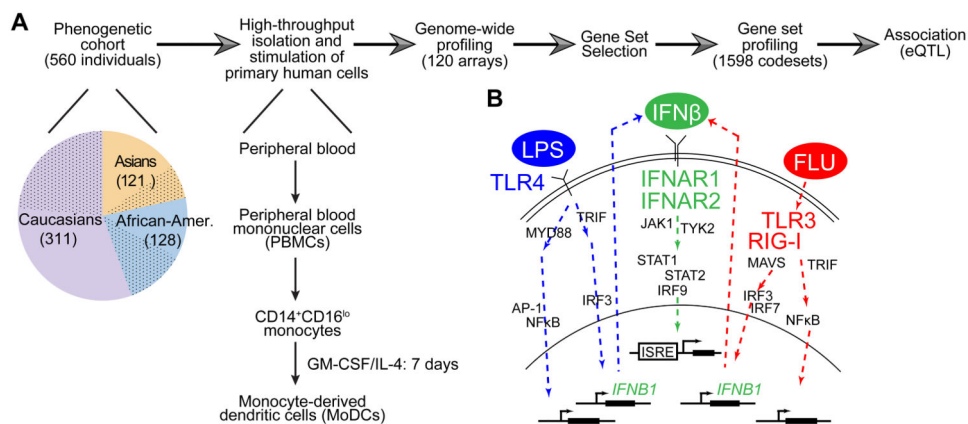


Fig. 1. A strategy to identify gene-by-environment interactions in the innate immune responses of primary human dendritic cells

(A) Strategy used to identify baseline and response expression quantitative trait loci (eQTLs and reQTLs), consisting of five steps: (i) high-throughput isolation and stimulation of primary human MoDCs from 560 healthy individuals (dotted slices, male; solid-colored slices, female) collected as part of the PhenoGenetic cohort; (ii) whole-genome gene expression measurements in a subset of the cohort; (iii) selection of signature gene set, consisting of regulators and regulated genes; (iv) digital multiplex gene expression measurements of signature genes in the entire cohort; and (v) mapping of genetic variation to expression variation. GM-CSF, granulocyte-macrophage colony-stimulating factor; IL-4, interleukin-4. (B) Model of innate immune pathways activated by three stimuli demonstrating their downstream relationships. Lipopolysaccharide (“LPS”) from *E. coli* engages the TLR4 receptor; interferon-beta (“IFNβ”) engages the heterodimeric IFNAR receptor; influenza A/PR8 (NS1) (“FLU”) engages the cytoplasmic TLR3 and RIG-I receptors. Receptor engagement activates signal transduction cascades that regulate expression of inflammatory genes, IFNs and IFN-stimulated genes. IFNAR activation also occurs during LPS and FLU stimulations because LPS and FLU both induce IFN production, leading to activation of ISREs. JAK1, Janus kinase 1.

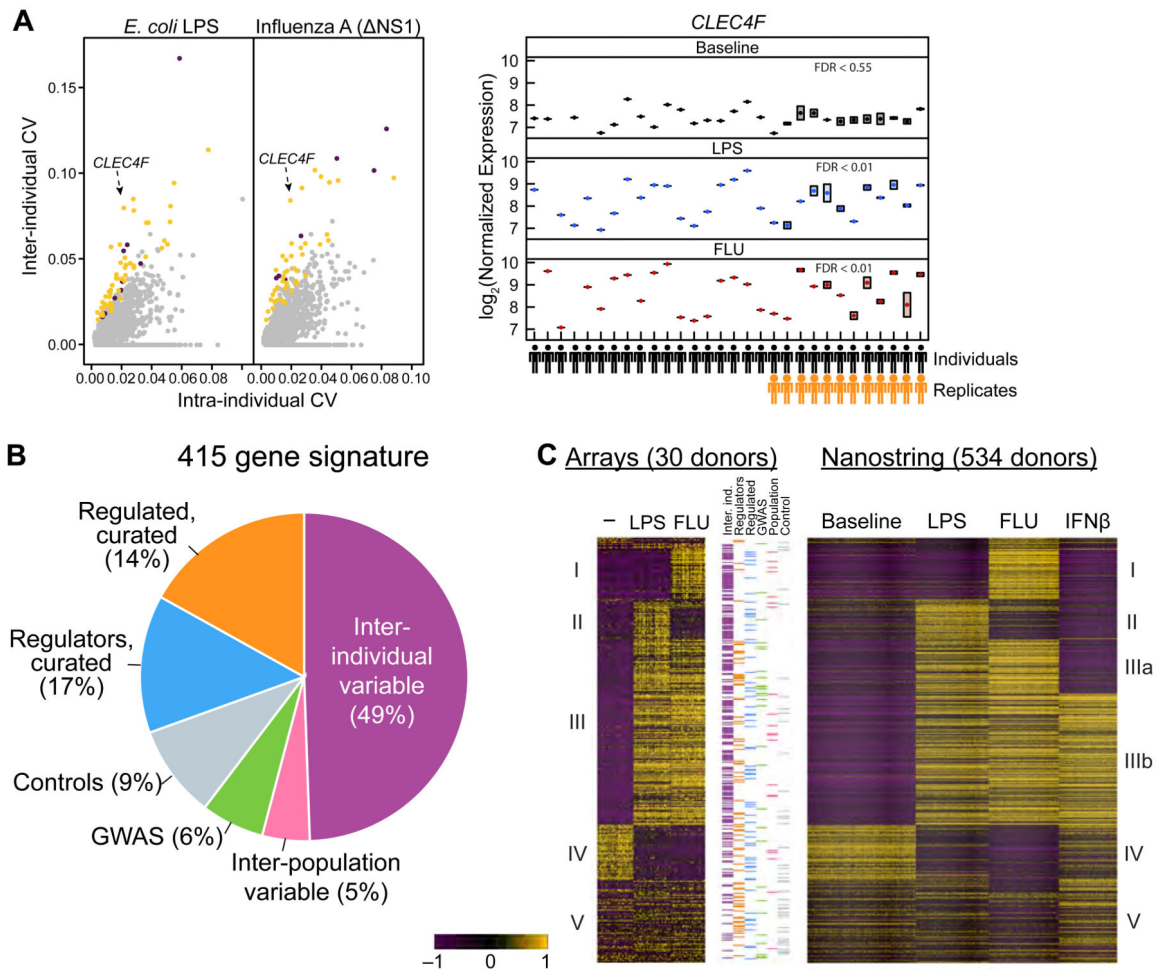


Fig. 2. Genome-wide expression profiles in MoDCs reveal response phenotypes

(A) Coefficient of variation (CV) of gene expression between 30 different donors (“Inter-individual CV”) plotted against CV of expression within 12 serial replicate samples (“Intra-individual CV”) for each differentially regulated (fold change >0.75 or <-1.5) gene following LPS or FLU stimulation. Yellow (up-regulated) and purple (down-regulated) circles represent genes with significant (moderated *t* test, FDR < 0.1) inter- vs. intra-individual variation. Right, log₂(expression, microarray data) of *CLECF* in baseline, LPS-stimulated and FLU-infected MoDCs from 30 donors and 12 replicates, demonstrating example of a gene that shows significant (FDR < 0.01) inter- vs. intra-individual variation following LPS and FLU stimulations but not at baseline (fig. S2B). Standard error of replicate samples (*n* = 12) is shown for each sample. (B) Pie chart of 415 signature genes selected for Nanostring codeset: 222 (49%) are regulated genes that showed significant (mixed model variance components test, permutation FDR < 0.1) inter- vs. intra-individual variability; 61 (14%) are curated, regulated genes with a known function in the innate immune response; 76 (17%) are curated regulators in the TLR4, TLR3, RIG-I and IFNAR pathways; 41 (9%) are control genes including low-variance genes, sex-specific genes and non-expressed genes; 28 (6%) are regulated genes that were reported in the regions of autoimmune and infectious disease GWAS; and 21 (5%) are regulated genes that showed

significant inter- versus intra-population variability. (C) Gene expression heatmap of the 415-gene signature in MoDCs from the microarray study (30 individuals) and the Nanostring study (534 individuals). Each row represents a gene; each column represents a donor sample at baseline, stimulated with LPS, infected with FLU or stimulated with IFN β . Rows were clustered by *k*-means clustering of Nanostring dataset with major clusters (I, II, IIIa, IIIb and IV) labeled. Between the two heat maps, each row was labeled with colored dashes corresponding to one of the 6 categories described in (B).

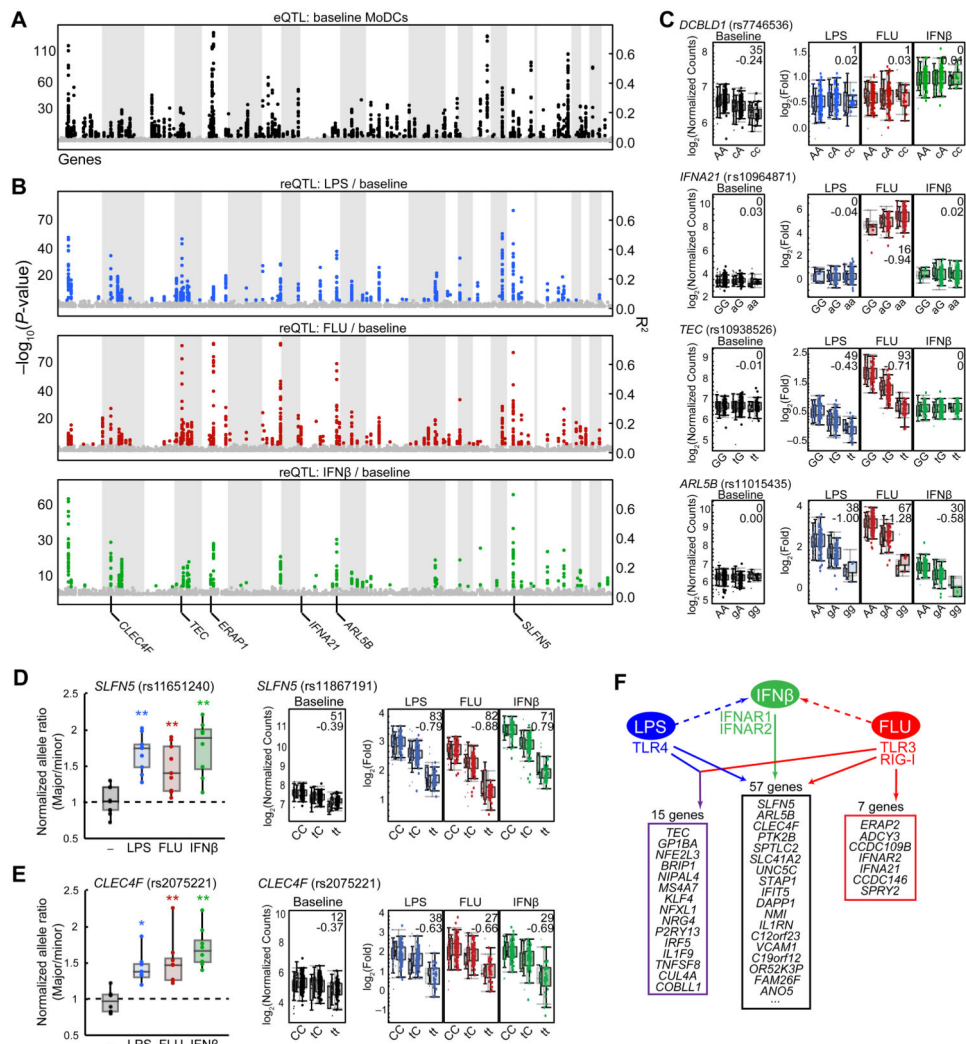


Fig. 3. Association analysis reveals cis-eQTLs and cis-reQTLs (A and B) Manhattan plot of cis-eQTLs (A, baseline expression) and cis-reQTLs (B, LPS-, FLU- and IFN β -stimulated fold changes relative to baseline) showing $-\log_{10}(P)$ values (left y axis) and R^2 values (right y-axis) for all cis-SNPs, which are displayed on the x-axis with associated genes ordered by their chromosomal location. (C) Box-whisker plots showing gene expression (left; $\log_2(\text{nCounts})$, y-axis) or fold change (right; $\log_2(\text{fold})$, y-axis) of *DCBLD1*, *IFNA21*, *TEC* and *ARL5B* in resting, LPS-stimulated, FLU-infected and IFN β -stimulated MoDCs as a function of genotype of the respective cis-SNPs (x-axis: rs27434, rs10964871, rs10938526 and rs11015435). African Americans, Asians and Europeans in this order are displayed as separate box-whisker plots adjacent to each other in each condition. $-\log_{10}(P)$ values) and β statistics are displayed in top right corners. (D and E) Allelic imbalance analysis of *SLFN5* (D) and *CLEC4F* (E) in resting, LPS-stimulated, FLU-infected and IFN β -stimulated MoDCs, showing the ratio of gene expression between the major and minor alleles in heterozygote (rs11651240 for *SLFN5*, rs2075221 for *CLEC4F*) cDNA samples ($n = 8$ in (D); $n = 9$ in (E)) normalized to the ratio in the corresponding genomic DNA samples; significant deviation from 1.0 (dashed line) is consistent with allelic

imbalance. Data are from one experiment representative of three (mean and standard deviation shown). * $P < 0.01$, ** $P < 0.001$, compared to unstimulated cells (Student's t -test). On the right panels, box-whisker plots showing expression (left; $\log_2(\text{nCounts})$, y-axis) or fold change (right; $\log_2(\text{fold})$, y-axis) of *SLFN5* (D) and *CLEC4F* (E) in resting, LPS-stimulated, FLU-infected and IFN β -stimulated MoDCs as a function of genotype of the respective cis-SNPs: rs11867191 and rs2075221. (F) Schematic showing the different combinations of stimuli leading to significant cis-reQTLs, with the most significant examples listed. Specificity to conditions was defined with M -value > 0.9 taken as the inclusion criteria and M -value < 0.1 taken as the exclusion criteria for each condition.

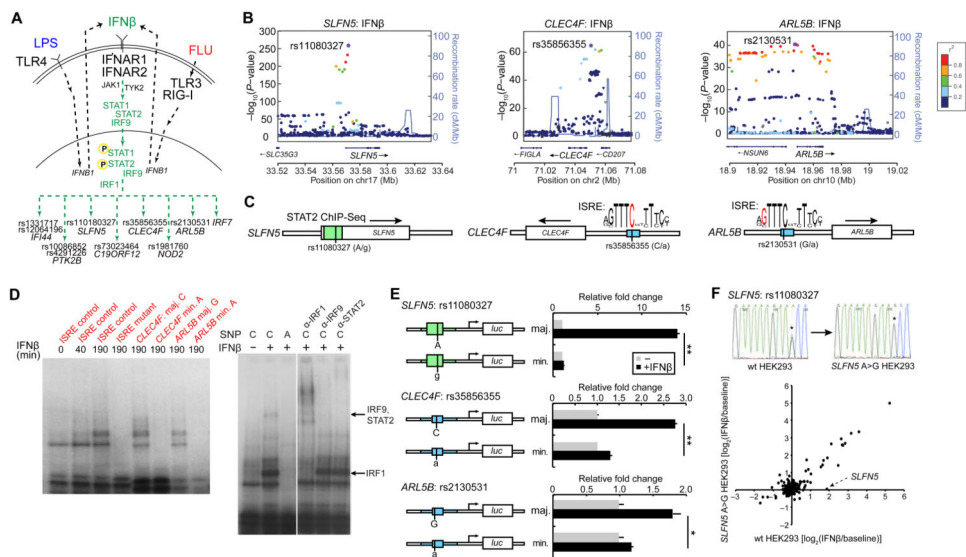


Fig. 4. Functional fine-mapping and mechanism of cis-reQTLs

(A) Pathway diagram of signal transduction cascade downstream of IFN β activation. Activation of receptor leads to downstream activation of JAK-STAT cascade, leading to posttranslational activation of STAT and IRF transcription factors. (B) LocusZoom plots showing the $-\log_{10}(P\text{-values})$ of imputed cis-eQTLs (y-axis) in the chromosomal regions (x axis) of *SLFN5*, *CLEC4F* and *ARL5B*. The most significant imputed SNPs in each locus are labeled. (C) Schematic representation of alleles in the regions near the *SLFN5*, *CLEC4F* and *ARL5B* genes that are in STAT2 ChIP-Seq binding sites or that perturb ISRE motifs (SNPs are shown as vertical bars and in red letters). (D) Electrophoretic mobility shift assays (EMSA) with 24- to 26-bp radiolabeled DNA probes—containing a known ISRE motif control, a mutated ISRE motif control, the *CLEC4F* rs35856355 major (C) or minor allele (A) sequences, or the *ARL5B* rs2130531 major (G) or minor allele (A) sequences—incubated with nuclear lysates from IFN β -stimulated MoDCs. On the right, supershift assays with or without antibodies against IRF1, IRF9, and STAT2 (designated α -IRF-1, and so on) with the *CLEC4F* rs35856355 major (C) probe are shown. (E) Luciferase expression from reporter constructs transfected into HEK293 cells that were left unstimulated or were stimulated with 1000 U/ml IFN β for 21 h. 150–200 bp sequences from the major and minor haplotypes of the *SLFN5*, *CLEC4F* and *ARL5B* regions were subcloned 5' of a minimal promoter and firefly luciferase gene. Firefly luciferase expression was normalized to *Renilla* luciferase expression expressed from cotransfected plasmid. (F) Fold change $\log_2(\text{IFN}\beta\text{stim}/\text{unstim})$ of signature genes in wild-type HEK-293 cells (rs11080327^{A/G}), plotted against fold change in CRISPR-converted (rs11080327^{G/G}) HEK-293 cells. Data are from one experiment representative of three (mean and standard shown in (E)). * $P < 0.05$, ** $P < 0.01$, compared to unstimulated cells (Student's *t*-test).

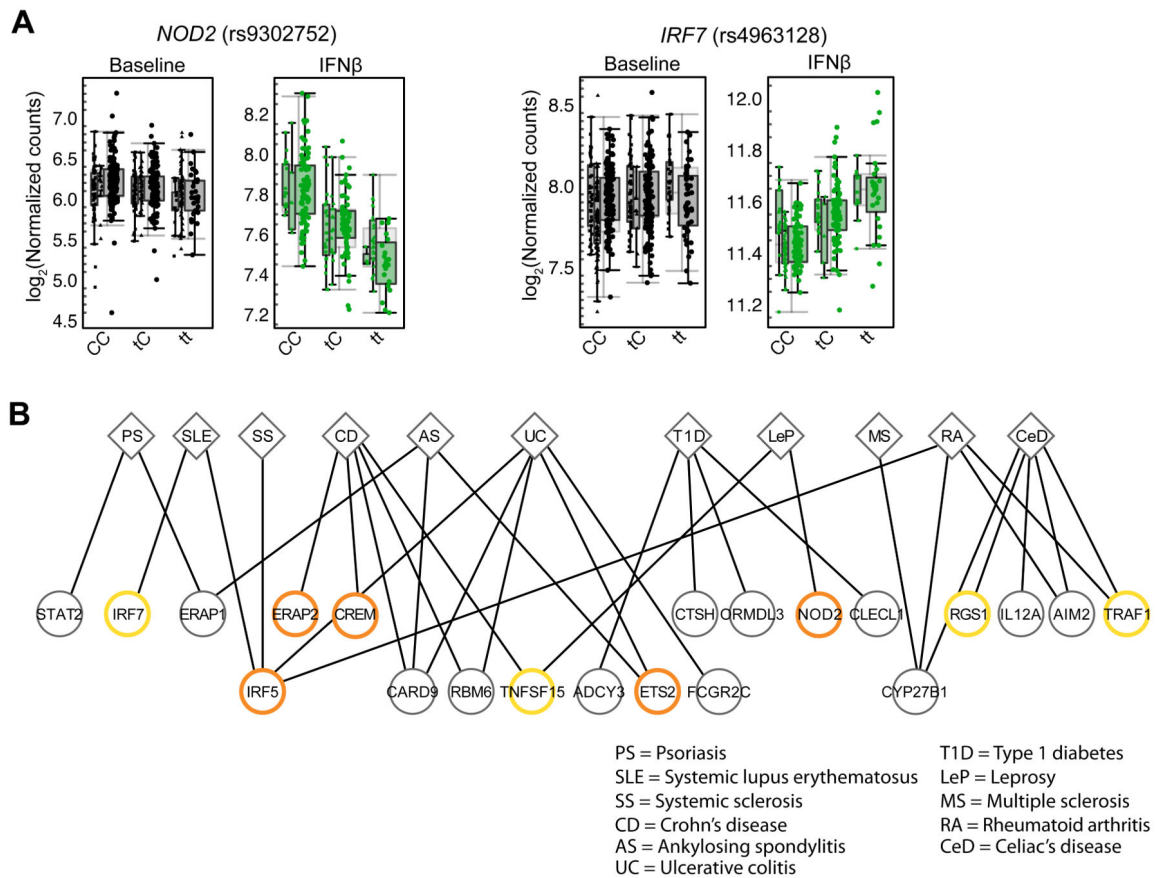


Fig. 6. Autoimmune and infectious disease-associated SNPs are cis-eQTLs and cis-reQTLs
(A) Expression ($\log_2(\text{nCounts})$) of *NOD2* in resting and IFN β -stimulated MoDCs from 184 Caucasians as a function of genotype of the leprosy GWAS SNP, rs9302752 (left). Right, expression ($\log_2(\text{nCounts})$) of *IRF7* in resting and IFN β -stimulated MoDCs from 184 Caucasians as a function of genotype of the SLE GWAS SNP, rs4963128. **(B)** Plot showing overlap of genome-wide significant ($P < 5 \times 10^{-8}$) GWAS SNPs with cis-eQTLs and reQTLs in MoDCs, with clinical phenotypes connected to corresponding gene expression phenotypes by lines. Orange circles represent cis-reQTLs ($P < 10^{-7}$); yellow circles represent stimulus-specific cis-eQTLs ($P < 10^{-7}$).